4. V. N. Kosov and Yu. I. Zhavrin, Diffusional and Convective Transport in Gases and Liquids [in Russian], Alma-Ata (1986), pp. 16-18.
5. V. N. Kosov and I. V. Bolotov, 4th All-Union Conference of Young Scientists and Specialists, "Current Problems of Thermal Physics," Summary of Documents, Novosibirsk (1986), pp. 25-26.
6. L. Miller and E. A. Mason, Phys. Fluids, 9, No. 4, 711-721 (1966).
7. L. Miller, T. H. Spurling, and E. A. Mason, Phys. Fluids, 10, 1809-1813 (1967).
8. B. A. Ivakin, P. E. Suetin, and G. S. Kharin, Tr. UPI, Sverdlovsk, No. 172, 154-156 (1969).
9. Yu. I. Zhavrin, N. D. Kosov, and Z. I. Novosad, Diffusion in Gases and Liquids [in Russian], Alma-Ata (1974), pp. 12-19.
10. S. M. Belov, Yu. I. Zhavrin, and N. D. Kosov, "Diffusional instability of a helium–argon–nitrogen gas mixture at different pressures and concentrations," Submitted to KazNIINTI 14.10.85, No. 1073, Alma-Ata (1985).

STUDY OF THE SYNCHRONICITY OF PRESSURE PULSATIONS IN FLUIDIZED-BED REACTORS

A. P. Baskakov, N. F. Filippovskii, V. G. Tuponogov, and A. V. Mudrechenko

UDC 66.096.5

The interrelation between pressure pulsations and the movement of gas bubbles in a fluidized bed is studied experimentally. Cross-correlation functions are presented for different points of a full-scale reactor.

An orderly theory of the development and propagation of pressure pulsations in fluidized beds has yet to be presented, despite the large number of studies [1-3] devoted to this subject. The creation of such a theory may be aided considerably by the study of correlations between the pressures at different points of a fluidized bed and the motion of gas bubbles in the bed.

The change which occurs in pressure with the passage of a gas bubble through a measurement point has been studied fairly well [3], and the experimental results obtained coincide with calculations such as those performed by the Davidson model [4]. The maximum pressure is seen at the moment the frontal point of the bubble approaches the sensor. Then pressure decreases until the sensor touches the rear point of the bubble. This can be clearly seen from Fig. 1 (points A_1-B_1 and A_2-B_2). If the bubble passes next to the sensor without touching it (the middle pressure maximum in Fig. 1), the pattern remains basically the same. The disturbing effect of the bubble is manifest at a distance on the order of the bubble's diameter from the axis of its rise.

The results shown in Fig. 1 were obtained in a planar transparent unit with a cross section of 18 × 300 mm. The heights of the fluidized bed H = 400-550 mm. The bed was maintained at the fluidization limit by supplying air through a perforated grate, while excess flow was directed through a central nozzle 5 mm in diameter. One of the pressure-sampling tubes was located next to the nozzle, while a second tube was located 0.44 m above the nozzle. The motion of the bubbles was monitored with photodiodes located at different elevations above the nozzle and illuminated through the bed. The current from all diodes and from the extensometric pressure sensors was recorded on an N338-6P multichannel recorder.

The character of pressure oscillation near the nozzle (Fig. 1c) was determined by the superposition of small-scale, high-frequency pulsations connected with the separation of small gas bubbles from the cavity and large-scale pressure gradients caused by the escape

S. M. Kirov Ural Polytechnic Institute. Translated from Inzhenerno-Fizicheskii Zhurnal, Vol. 55, No. 1, pp. 97-102, July, 1988. Original article submitted February 18, 1987.

 0022-0841/88/5501-0778 $12.50

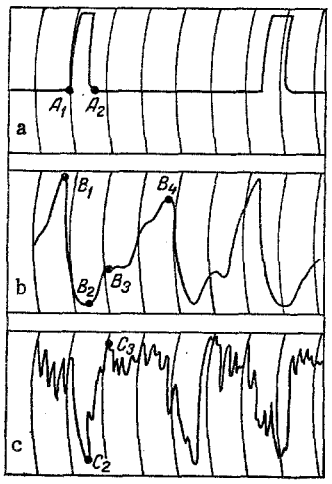

Fig. 1

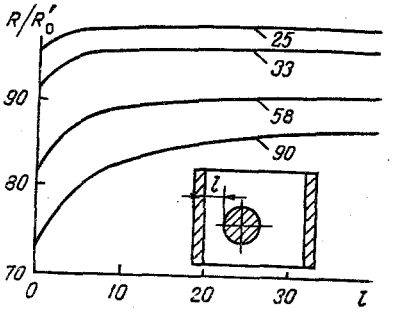

Fig. 2

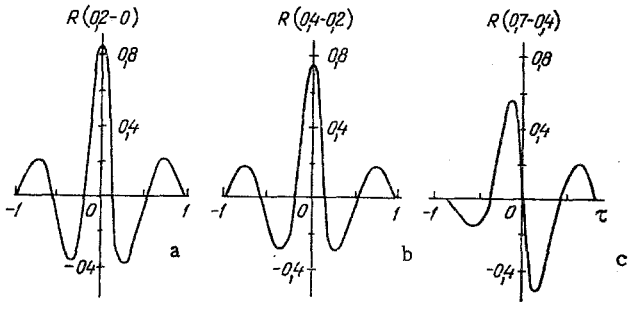

Fig. 3

Fig. 1. Oscillograms of the photodiode current (a) and the pressure pulsations 0.44 m above the nozzle (b) and just below the nozzle (c): H = 0.52 m.

Fig. 2. Change in the relative resistance of the model with increasing distance of the cylindrical cavity from one of the electrodes; the numbers next to the curves denote the diameter of the cavity in mm. R/R_0', %; ℓ, mm.

Fig. 3. Cross-correlation function of pressure pulsations at points lying on one vertical at the elevations: 0.2-0 m (a); 0.4-0.2 (b); 0.7-0.4 (c); H_0 = 0.8 m; W = 2.6; corundum d = 0.4 mm. τ, sec.

of the bubbles to the surface. The reduction in pressure in the lower region of the bed with the escape of a bubble to the surface occurs mainly as a result of the associated change in the permeability of the bed. To evaluate this, we modeled a two-dimensional bed with a circular cavity on electrically conducting paper. This method was suggested in [5], where it was found that the rate of gas flow through the cavity increases as it approaches the surface of the bed. In the present case, we monitored the change in the total resistance of electrically conducting paper of the width B = 160 mm and length L = 160 mm with the displacement of metal rings of different diameters D (Fig. 2) along the axial lines of the model from one electrode to another. This corresponded to a change in the fluid resistance of the two-dimensional bed as a cylindrical bubble ascends in it. To account for the change in the height of the bed (and, accordingly, resistance) due to the introduction of a gas bubble into the bed, we referred the measured resistance of the model not to the initial resistance R_0, but to a somewhat lower value

$$R_0' = R_0(1 - \pi D^2/4BL).$$

It is evident from Fig. 2 that as the bubble approaches the surface, the resistance of the bed decreases considerably, and deep in the bed even bubbles which are coarse relative to the size of the bed have almost no effect on bed resistance.

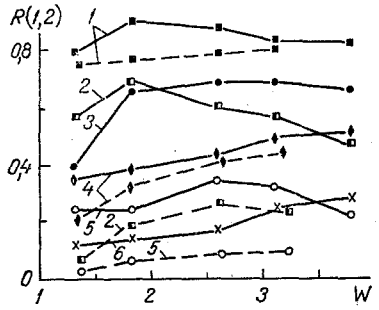

Fig. 4. Dependence of values of the cross-correlation function linking fluidization velocity and pressure pulsations, with τ = 0, at points 0.7 m apart and at the same level: 1, 3, 4, 6) H = 0.8 m; 2, 5) H = 0.3; 1, 2) h = 0; 3, 5) 0.2; 4) 0.4; 6) 0.7 m. The solid lines correspond to φ = 2.4%, the dashed lines correspond to φ = 0.75%.

There is one more reason for the reduction in pressure under the bed as a bubble leaves it – acceleration of the bed material. The gas enters the bed relatively uniformly through the grate and nozzle, while it leaves in pulses, with the maximum flow rate corresponding to the moment the gas bubble reaches the surface. This follows from the two-dimensional model of the bed and is confirmed by the experiments in [6]. As a result of the formation and rise of bubbles in the bed, gas accumulates in the bed and the height of the bed increases. When the bubble reaches the bed surface, bed height suddenly decreases – the bed is accelerated. The inertia of the particles helps reduce the pressure under the bed.

The analysis of many oscillograms similar to those presented in Fig. 1 showed that the pressure under the bed (at the nozzle) begins to decrease when the bubble is a distance from the bed surface which is roughly equal to the height of the bubble. This decrease in pressure is accompanied by swelling of the bed surface above the bubble and a corresponding increase in gas velocity above the bed. As follows from Fig. 2, the lowest pressure under the bed is seen when the frontal point of the bubble touches the bed surface.

For Fig. 1, we specially chose the case in which the height of the bubble is roughly equal to the distance from the upper pressure-measurement point to the bed surface $H_b \sim H - h_g$ = 8 cm. In this case, the pressures in the top and bottom regions of the bed decrease synchronously (points B_2-C_2), although the physical reasons for the pressure pulsations are different. The causes of the pulsations are the passage of the bubble through the measurement point in the case of the top sensor and the overall reduction in pressure in the bed in the case of the bottom sensor.

After the gas bubble leaves the bed, the pressures at the measurement points are established at the levels corresponding to the hydrostatic pressures (points B_3-C_3). Meanwhile, below these points, the value is close to the maximum. Above the points, the approach of the next bubble toward the measurement point leads to a large further increase in pressure (point B_4). This increase is connected with a higher rate of filtration of the gas through the bubble.

The physical pattern described above allows us to better interpret the results of statistical analysis of pressure pulsations in a fluidized bed. According to our data and to the results presented in [1], pressure pulsations in the lower half of the layer occur nearly in synchrony – and even slightly in advance in the middle of the bed – relative to the pulsations at the lowest level next to the grate. Only above the middle of the bed is it noticeable that the pressure pulsations at the upper points lag behind the pulsations at lower points by the time period $\Delta\tau$, corresponding to the time of movement of the bubbles between measurement points. Such data was obtained not only under laboratory conditions, but also in commercial-scale units (Fig. 3) 0.6 × 1.2 m in plan with a bed height H_0 = 0.8 m. A description of this unit and the measurement method can be found in [2, 7]. The cross-correlation function for the pressure pulsations $R(\tau)$ at different points on a single vertical in the lower half of the bed has a maximum with a time shift τ = 0 (Fig. 3a and b). This means that the pressure oscillations at these points occur synchronously, although they do not exactly repeat one another – since $R(\tau)_{max} \approx 0.8$ with a distance of 0.2 m between the measurement points. The pressure pulsations at the 0.7-m and 0.4-m elevations are noticeably phase-shifted (Fig. 3c).

When a sensor is placed at the upper level of the bed, pressure near it and near the grate changes in opposite phase, since pressure near the upper sensor increases only during the swelling of the surface by the bubble, while pressure is simultaneously decreasing near the grate.

TABLE 1. Values of the Cross-Correlation Function $R_{max}(i, j)$, with $\tau = 0$, for the Pressure Pulsations at Different Points of the Gas-Distributing Grate

j	i		
	P_1	$P'-P_1$	P'
Pressure above the grate at point 1 P_1	1	—	0,75
Pressure drop over the gas flow meter in the cap at point 1 ΔP_1	—0,55	0,82	—0,6 (τ=0,038)
Pressure in the subgrate chamber P'	0,75	—	1
Pressure above the grate at point 2 at a distance of 0,7 m from point 1 P_2	0,62	—	0,74
Pressure drop over the gas flow meter in the cap at point 2 ΔP_2	—0,15	0,05	—0,57 (τ=0,038)

Note. The parentheses show nontrivial values of τ, sec. φ = 2.4%, H_0 = 0.3 m, W = 2.6.

In reactors with a large area, the pressure pulsations across the reactor may become quite asynchronous due to the formation of several preferred bubble-escape zones [8]. As a simplification, we can represent each such zone as an individual reactor with an area $S \sim H^2$. Each of these individual reactors shares the same sub-grate chamber. The criterion for classifying a reactor as "large" is the condition $S_{re} \gg H^2$. For a reactor with an area of 1.2 × 0.6 m, this condition is satisfied at H = 0.3 m, while it is not satisfied at H = 0.8 m.

The small values of the cross-correlation coefficients at points 1 and 2, located in the upper region of the bed fairly far apart from each other (0.7 m) along a diagonal in a horizontal section of the unit (Fig. 4, curves 5 and 6), indicate that the bubbles in each zone leave the bed independently. The escape of a bubble leads to a drop in pressure over the entire height of the given zone and to an increase in the rate of gas flow through the grate in this zone. Evidence of this is the rather large negative value of the cross-correlation coefficient of pressure above the grate P_1 and the pressure gradient ΔP_1 on the convergent duct (Venturi nozzle) installed in the top of the cap located near pressure-measurement point 1 above the grate (Table 1). Due to the increase in the rate of gas flow through the grate, the pressure drop in the subgrate chamber P' naturally occurs with a certain lag relative to the flow-rate change (ΔP_1 and ΔP_2).

A reduction in the pressure under the grate lowers the pressure in the entire lower region of the bed. Thus, the pressure pulsations P_1 and P_2 are nearly synchronous (curves 1 and 2 in Fig. 4). The degree of synchrony is even greater with the pressure pulsations in the subgrate chamber P' (Table 1). The connection established through the chamber is of course weakened by an increase in the resistance of the grate (see Fig. 4, solid and dashed lines 2 and 5). With a large value of bed height H_0 = 0.8, a change in the resistance of the grate does not significantly affect the correlation of the pressure pulsations at different points of the lower bed region, since the effect of the bubbles leaving the bed is distributed over the entire lower section of the bed.

In reactors of large cross section with a gas-distributing grate having a low resistance, the subgrate chamber performs the role of synchronizer of the pressure pulsations across the reactor. As a result, when the volume of the subgrate chamber is large and the resistance of the grate is low, a relaxational oscillatory regime may develop. Here, material will be periodically deposited on the grate, even in reactors with a very large cross section [9]. Such regimes were studied in detail in [10] for small reactors, and the authors correctly noted that their occurrence requires a force which can keep the bed stationary and produce an increase in pressure under the stationary bed greater than $P_0 = \rho g H_0$. The authors of [10] believe that wall friction may play such a role.

In large reactors (a reactor of 100 m^2 area was described in [9]), wall friction cannot make such a large contribution. The actual reason for the appearance of the pressure peak on the fluidization curve P = f(w) is the resistance ΔP_{add} connected with redistribu-

tion of the gas flow leaving the holes in the grate over the entire cross section of the bed corresponding to the given hole [11]. After the transition to the fluidized state, the bed is thrown up above the grate and $\Delta P_{add} \to 0$. A method of calculating ΔP_{add} was proposed in [11]. This makes it possible to calculate the conditions for onset of the oscillatory regime in large reactors (such as in [10]) and to take steps to eliminate them, since they have many undesirable consequences: deformation of the grate, falling of material through the grate.

Confirmation that a change in the resistance of the grate is responsible for the oscillations is the sharp increase in the mean value of grate resistance during the oscillatory regime. According to the data in [9], a "dry" grate has a resistance of 0.3 kPa, while the resistances of the grate in the bubble and oscillatory regimes are 0.5 kPa and 1.3 kPa, respectively.

Incidentally, the resistance of the gas-distributing grate is also variable during bubble fluidization. This is evidenced by the difference [R(i, j) = 0.82 in Table 1] in the pressure-gradient pulsations at the flow-rate meter in the cap ΔP_1 and the pressure gradient in the cap as a whole $P' - P_1$.

NOTATION

B, width of the electrically conducting model; D, diameter of the metal ring; d, diameter of the particles; g, acceleration due to gravity; H, h, height of fluidized bed, elevation in the bed above the gas-distributing grate; L, ℓ, length of the electrically conducting model, running length of the model; P, ΔP, pressure, pressure gradient; R(i, j), normalized cross-correlation function; S, cross-sectional area of the unit; ρ, density of the finely dispersed material; φ, relative cross-sectional area; τ, time of shift of cross-correlation function; W, fluidization number. Index 0, at the fluidization limit.

LITERATURE CITED

1. L. T. Fan, Ho Tho-Ching, S. Hiraoka, and W. P. Walawender, AIChE J., 27, No. 3, 388-396 (1981).
2. A. P. Baskakov, V. G. Tuponogov, and N. F. Filippovskii, Inzh.-Fiz. Zh., 45, No. 3, 423-426 (1983).
3. V. G. Kul'bachnyi and K. E. Makhorin, Inzh.-Fiz. Zh., 21, No. 6, 998-1004 (1971).
4. I. F. Davidson and D. Harrison, Fluidization of Solid Particles [Russian translation], Moscow (1965).
5. N. I. Gel'perin, G. I. Lapshenkov, V. P. Karmannikov, and V. G. Ainshtein, Khim. Mashinstr., Moscow, 6, 41-46 (1976).
6. D. R. McGow, Chem. Eng. Sci., 32, 11-18 (1977).
7. A. P. Baskakov, V. G. Tuponogov, and N. F. Filippovskii, Inzh.-Fiz. Zh., 43, No. 3, 357-360 (1982).
8. N. I. Gel'perin (ed.), Fluidization [Russian translation], Moscow (1974).
9. E. A. Kazakova, Granulation and Cooling of Nitrogen-Bearing Fertilizers, Moscow (1980).
10. V. A. Borodulya, Yu. A. Buevich, and V. V. Zav'yalov, Inzh.-Fiz. Zh., 30, No. 3, 424-433 (1976).
11. A. P. Baskakov, N. F. Filippovskii, and V. G. Tuponogov, Khim. Neft. Mashinostr., No. 11, 22-24 (1985).